

# LMC self lensing for OGLE-II microlensing observations

S. Calchi Novati<sup>1,2,3</sup> \*, L. Mancini<sup>1,2,3</sup>, G. Scarpetta<sup>1,2,3</sup> and Ł. Wyrzykowski<sup>4</sup>

<sup>1</sup> Dipartimento di Fisica “E. R. Caianiello”, Università di Salerno, Via S. Allende, 84081 Baronissi (SA), Italy

<sup>2</sup> Istituto Nazionale di Fisica Nucleare (INFN), Sez. di Napoli, Italy

<sup>3</sup> Istituto Internazionale per gli Alti Studi Scientifici (IIASS), Vietri Sul Mare (SA), Italy

<sup>4</sup> Institute of Astronomy, University of Cambridge, Madingley Road, Cambridge CB3 0HA, UK

date

## ABSTRACT

In the framework of microlensing searches towards the Large Magellanic Cloud (LMC), we discuss the results presented by the OGLE collaboration for their OGLE-II campaign (Wyrzykowski et al. 2009). We evaluate the optical depth, the duration and the expected rate of events for the different possible lens populations: both luminous, dominated by the LMC self lensing, and “dark”, the would be compact halo objects (MACHOs) belonging to either the Galactic or to the LMC halo. The OGLE-II observational results, 2 microlensing candidate events located in the LMC bar region with duration of 24.2 and 57.2 days, compare well with the expected signal from the luminous lens populations:  $n_{\text{exp}} = 1.5$ , with typical duration, for LMC self lensing, of about 50 days. Because of the small statistics at disposal, however, the conclusions that can be drawn as for the halo mass fraction,  $f$ , in form of compact halo objects are not too severe. By means of a likelihood analysis we find an *upper* limit for  $f$ , at 95% confidence level, of about 15% in the mass range ( $10^{-2} - 10^{-1}$ )  $M_{\odot}$  and 26% for  $0.5 M_{\odot}$ .

**Key words:** Galaxy: Structure, Halo; Galaxies: Large Magellanic Cloud; Physical data and processes: Gravitational Lensing; Cosmology: Dark matter

## 1 INTRODUCTION

Following the original suggestion of Paczyński (1986, 1991), only a few years later, the MACHO, EROS and OGLE collaborations started their observational microlensing campaign towards the LMC and the Galactic bulge with the aim of probing, in particular as for the first line of sight, the Galactic dark matter distribution in form of MACHOs. After the first exciting detection of microlensing events, (Alcock et al. 1993; Aubourg et al. 1993; Udalski et al. 1993), by now the statistics of detected microlensing candidates allows one to begin to draw conclusions on the relevant scientific issues of interest. As for the lines of sight towards the LMC, the MACHO and the EROS collaborations have presented the final results of their several-years campaigns, getting to altogether different conclusions as for the content of the Galactic halo in compact halo objects. The MACHO collaboration (Alcock et al. 2000) have presented 13-17 microlensing candidate events and have evaluated an optical depth  $\tau = 1.2_{-0.3}^{+0.4} \times 10^{-7}$ , far larger than what is expected from the known possible luminous lens populations. Their analysis indicates that a mass fraction of about 20% of the dark matter halo should be composed by MACHOs in the preferred mass range (0.15 – 0.9)  $M_{\odot}$ . On the other hand, the analysis of the EROS collaboration leads to a different conclusion. No viable

microlensing candidate event have been detected, and accordingly EROS have evaluated a rather tight *upper* limit for the fraction of compact halo objects. In particular they evaluate an upper limit for the optical depth, due to such lenses,  $\tau < 0.36 \times 10^{-7}$  (95% confidence level). This translates, in particular, in an upper limit of about 8% for the halo mass fraction in form of  $0.4 M_{\odot}$  compact halo objects (Tisserand et al 2007).

The strategies followed by the MACHO and the EROS collaborations are different. EROS covered a larger sky region around the LMC and considered as potential sources only a subset of clearly identified “bright” stars following the successful approach used for Galactic bulge searches (Popowski et al. 2005; Hamadache et al. 2006; Sumi et al. 2006); whereas MACHO concentrated the observations along the LMC bar region, where the contamination to “MACHO lensing” (lensing events due to lenses belonging to the dark matter halo population in form of compact objects) by self lensing (lensing events with the lens belonging to the same luminous population as the source star) is expected to be larger, and kept as viable sources also blended objects. This does not seem to be sufficient, however, to account for the difference in their results, and indeed several explanations have been proposed to understand the nature and the location of the lens for the observed MACHO microlensing candidates. First, it should be noted that it is likely that the lenses do not all belong to the same population (Jetzer et al. 2002). In particular, the LMC self lensing has

\* E-mail: novati@sa.infn.it

been proposed (Sahu 1994; Wu 1994; Gyuk et al. 2000) as a viable solution, but Mancini et al. (2004) have shown that it can not explain most of the events. Calchi Novati et al. (2006) have studied the possibility for some of the lenses to belong to the LMC dark matter halo (a similar possibility, but for observations towards the SMC, have also been considered by Dong et al 2007). Finally, two candidates have been acknowledged to belong to the Galactic disc (Alcock et al. 2001; Kallivayalil et al. 2006). In fact, the possibility that some of the microlensing candidates are not microlensing variation at all must be taken into account. Recently Bennett (2005) has refined and put up to date the selection of the MACHO events, taking into account the possible contamination of variable stars. As a result, 10-12 out of the original set of the 13 “set A” variations (Alcock et al. 2000) are acknowledged as “likely to be microlensing events”, with a resulting new estimate of the microlensing optical depth  $\tau = (1.0 \pm 0.3) \times 10^{-7}$ , still in agreement with the previous one, and such that the overall conclusions of this new analysis do not differ substantially from that of the original MACHO analysis.

In this paper we discuss the recent observational results presented by Wyrzykowski et al. (2009) for the OGLE-II campaign towards the LMC. In particular, we carry out a detailed evaluation of the expected lensing signal due to the different luminous populations as opposed to MACHO lensing. The paper is organised as follows. In Section 2 we describe the models for the different lens populations that may give rise to microlensing events along this line of sight. In Section 3 we present our analysis based on the evaluation of the microlensing quantities, the optical depth and the microlensing rate, and discuss our results as compared to the observational results of the OGLE campaign.

## 2 MODELS

### 2.1 The LMC

The LMC luminous components, the *disc* and the *bar*, are modelled following the analysis presented in a series of papers by Van der Marel and co-authors (van der Marel & Cioni 2001; van der Marel 2001; van der Marel et al. 2002). The disc and the bar are considered to be both centered at  $\alpha = 5^{\text{h}} 27.6^{\text{m}}$ ,  $\delta = -69.87^\circ$  (J2000) at a distance of  $D = 50.1$  kpc. We assume a bar mass of  $M_{\text{bar}} = 1/5 M_{\text{disk}}$  (Sahu 1994; Gyuk et al. 2000), with a total visible mass in disk and bar of  $M_{\text{bar}} + M_{\text{disk}} = (2.7 \pm 0.6) \times 10^9 M_{\odot}$  (van der Marel et al. 2002). The intrinsic shape of the LMC disc is elliptical, with an inclination angle of  $34.7^\circ$ . The disc vertical distribution is described by a  $\text{sech}^2$  function, with a flaring height scale of about 0.3 kpc. We use a scale length for the disc exponential planar distribution of 1.54 kpc, and a boxy shaped bar (Zhao & Evans 2000) with length and height scale of 1.2 kpc and 0.44 kpc, respectively. Further details are given in Mancini et al. (2004).

For the velocity distribution, we assume a gaussian isotropic profile with line of sight velocity dispersion of 20.2 km/s (van der Marel et al. 2002) for disc stars (acting both as sources and lenses) and 24.7 km/s (Cole et al. 2005) for bar stars (sources and lenses). A detailed study of the deviation from this functional form may be found in Mancini (2009).

The lens mass function is a crucial ingredient as it constitutes the link between the number of available lenses and the overall mass of the luminous component under consideration. We use (Kroupa 2002, 2008) a broken power law  $\xi(\mu_l) \propto \mu_l^{-\alpha}$  with

$\alpha = 1.3, 2.3$  in the mass ranges  $(0.08, 0.5) M_{\odot}$  and  $(0.5, 1) M_{\odot}$  respectively ( $\mu_l$  is the lens mass). For  $\mu_l > 1 M_{\odot}$  we use the present day mass function (PDMF) value  $\alpha = 4.5$  and we normalize the overall mass in the mass range up to  $120 M_{\odot}$ . In fact, most of the mass is given by objects with mass smaller than  $1 M_{\odot}$  but the use of the PDMF value ensure us the correct normalization in each mass range. The maximum value for the lens mass should be fixed, once given the threshold magnitude for the sources (in the present case  $I = 20.4$ , Wyrzykowski et al. 2009), according to the demand for the lens to be an unresolved object. Therefore, taking into account the lens distance, the mass-luminosity relationship and the (varying) extinction conditions of the specific line of sight (Subramaniam 2005), we fix this value at  $2 M_{\odot}$  (for a resulting average lens mass of  $\langle \mu_l \rangle \sim 0.32 M_{\odot}$ ). However, we find our results to be quite insensitive to this choice: moving this limit up to  $5 M_{\odot}$  the overall expected number of events rises only by about 5%. In principle we might include also a sub-stellar component extending the lens mass range in the brown dwarfs regime down to  $0.01 M_{\odot}$ . Recent studies (Thies & Kroupa 2007) suggest a flattening in the mass function slope,  $\alpha = 0.3$ , so that we would find, for the expected number of events, an increase of only about 4%. It is worth recalling that these parametrizations are based on analyses carried out within our Galaxy. Robust results from analyses carried out within the LMC itself are still missing, in particular for stars with mass below  $0.4 M_{\odot}$  (in fact the most interesting mass range for our purposes) even if a few first analyses show roughly consistent, although somewhat steeper, behaviours (Gouliermis et al. 2006; Da Rio et al. 2009).

A further “luminous”, even if somewhat elusive, component that can be considered as a potential lens population is that of the *stellar halo* (SH) of the LMC. As a fiducial model we include this contribution following the analysis of Alves (2004) with the parametrization as given in Calchi Novati et al. (2006). In particular we attribute to the stellar halo, endowed with a *spherical* mass distribution, a total mass, within 8.9 kpc of  $0.35 \times 10^9 M_{\odot}$ . Based on a new analysis of OGLE-III RR Lyrae stars, Pejcha & Stanek (2009) suggested, instead, a *triaxial ellipsoid* mass distribution for the stellar halo, elongated along the line of sight to the observer. As a test model we follow their parametrization, using the same functional distribution and total mass as in Alves (2004), with a position angle of  $112.4^\circ$  and an inclination angle of  $6^\circ$ , axes ratio 1 : 2.0 : 3.5 and FWHM length along the line of sight of 7.56 kpc. Since the microlensing rate is proportional, through the Einstein radius, to the lens-source distance, the expected signal from the stellar halo can become relatively large in spite of the overall small total mass of this component. For the velocity distribution we use a gaussian isotropic profile with line of sight velocity dispersion of 53 km/s (Minniti et al. 2003; Borissova et al. 2006).

The total dynamical mass of the LMC,  $8.7 \times 10^9 M_{\odot}$ , as compared to the discussed luminous components, requires that more than half of it be comprised in a dark matter halo component (van der Marel et al. 2002). To study the possible contribution of LMC MACHO objects to the lensing signal we assume a isothermal spherical density profile with core radius of 2 kpc (Alcock et al. 2000) and a velocity dispersion of 46 km/s (van der Marel et al. 2002).

### 2.2 The Milky Way

Along the line of sight towards the LMC, the Milky Way (hereafter MW) provides two further luminous lens populations: the disc and the stellar halo. For the *disc* density distribution we fol-

**Table 1.** Characteristics of the two OGLE-II events observed towards the LMC (data taken from Wyrzykowski et al. 2009).

event	RA [J2000.0]	Dec [J2000.0]	$t_E$ days	$\tau \times 10^{-8}$
OGLE-LMC-1	5:16:53.26	-69:16:30.1	57.2	2.8
OGLE-LMC-2	5:30:48.00	-69:54:33.6	24.2	1.6

low the parametrisation of the model discussed in Han & Gould (2003) and modified as discussed in Calchi Novati et al. (2008). We use a length scale for the exponential profile of 2.75 kpc and a height scale (sech<sup>2</sup> model including a flare) of 0.25 kpc. Given the mass function as a power law including the brown dwarf mass range we fix the local density in agreement with local star counts at  $\Sigma_0 \sim 25 M_\odot$  (Kroupa 2002, 2007). We use a gaussian isotropic velocity distribution with line of sight velocity dispersion of 30 km/s. As for the Galactic *stellar halo* mass function and overall normalization we follow the analysis of Chabrier (2003). In particular we consider stars up to a mass of 0.9  $M_\odot$  with a local normalization of  $9.4 \times 10^{-5} M_\odot \text{pc}^{-3}$ . We use a mass distribution with a  $\rho \propto r^{-3}$  radial profile with flattening 0.6 and line of sight velocity dispersion of 120 km/s (Helmi 2008).

Besides the luminous lens populations, the largest contribution to the microlensing rate towards the LMC is expected to come from the would be MACHOs belonging to the Galactic dark matter halo. For this component we use the “standard” isothermal spherical density profile with core radius of 5 kpc (Alcock et al. 2000), local density of  $7.9 \times 10^6 M_\odot \text{kpc}^{-3}$  and 155 km/s as the value for the line of sight velocity dispersion. For MACHOs (in both halos) we consider a set of delta function in the mass range ( $10^{-5} - 10$ )  $M_\odot$ .

Throughout the paper we assume a value for the distance to the Galactic centre of 8 kpc (Trippe et al. 2008; Groenewegen et al. 2008; Gillessen et al. 2009).

### 3 ANALYSIS

#### 3.1 The OGLE-II results

Wyrzykowski et al. (2009) presented the final results of the OGLE-II campaign towards the LMC. The monitored fields are concentrated along the LMC bar region (covering a somewhat smaller region than the MACHO fields). The observational campaign lasted 1428 days through 4 years (1996-2000). The search for microlensing events has been carried out working both with a larger set of possible source of even blended objects and with a subsample of “bright” sources only, to which we refer to, following Wyrzykowski et al. (2009), as *All* and *Bright* star samples, respectively. As a result, from the first set of sources two microlensing candidate events have been detected, whose characteristics are summarised in Table 1, and none from the second restricted sample. The optical depth evaluated for the *All* sample sums up to  $\tau_{\text{obs}} = (4.3 \pm 3.3) \times 10^{-8}$ .

The observational strategy of this OGLE-II campaign towards the LMC has been more similar to that followed by the MACHO collaboration: both for the choice of the target fields, concentrated along the LMC bar, where the self-lensing contamination to the MACHO signal is expected to be larger, as well as for the sample of possible source objects, with the (delicate) issue of blending to be dealt with. (Concerning blending, Wyrzykowski et al. (2009) carried out a thorough analysis, in particular by making use of some HST LMC-fields luminosity functions, in order to correctly eval-

**Table 2.** Values of the optical depth ( $\tau \times 10^{-8}$ ) towards the centre of the 21 OGLE-II fields, and the two microlensing events, for the LMC lens populations considered in the paper: self lensing (SL), stellar halo and MACHO lensing (dark halo). For stellar halo we report both the results obtained using the spherical and (in brackets) the ellipsoidal model. RA and DEC are in degree (J2000.0).

field	RA	DEC	SL	stellar halo	dark halo
1	83.45	-70.10	4.36	0.591 (1.411)	6.01
2	82.82	-69.86	4.45	0.621 (1.405)	6.09
3	82.20	-69.80	4.65	0.651 (1.379)	6.20
4	81.57	-69.80	4.78	0.678 (1.340)	6.32
5	80.95	-69.68	4.63	0.679 (1.254)	6.37
6	80.33	-69.62	4.37	0.671 (1.162)	6.40
7	79.70	-69.40	3.89	0.629 (1.026)	6.33
8	79.07	-69.32	3.44	0.599 (0.925)	6.29
9	78.45	-69.23	2.98	0.564 (0.829)	6.24
10	77.82	-69.15	2.53	0.530 (0.742)	6.17
11	77.17	-69.17	2.14	0.510 (0.681)	6.16
12	76.57	-69.64	1.50	0.611 (0.749)	6.91
13	76.56	-68.72	1.67	0.427 (0.551)	5.77
14	75.95	-69.08	1.52	0.461 (0.565)	6.07
15	75.32	-69.08	1.28	0.445 (0.523)	6.07
16	84.07	-70.16	4.00	0.549 (1.373)	5.87
17	84.70	-70.28	3.58	0.507 (1.314)	5.72
18	85.32	-70.41	3.12	0.466 (1.240)	5.58
19	85.95	-70.58	2.64	0.430 (1.156)	5.45
20	86.57	-70.75	2.20	0.400 (1.072)	5.33
21	80.31	-70.56	1.95	0.954 (1.539)	7.88
1	79.22	-69.27	3.45	0.596 (0.932)	6.27
2	82.70	-69.91	4.60	0.632 (1.410)	6.13

uate the number of available sources). Because of this reason, a comparison with the results of the MACHO collaboration is more straightforward. However, as we detail below, it turns out that the results of OGLE are rather in agreement with those obtained by the EROS collaboration, which followed a different strategy (monitoring a much larger area of the sky and considering a subsample of bright stars for the analysis only).

#### 3.2 The microlensing quantities

To analyse the microlensing signal we start from the evaluation of the microlensing quantities, the optical depth and the microlensing rate (e.g. Roulet & Mollerach 1997). We recall that the optical depth allows one to characterise the overall lens mass distribution, without giving, however, informations on any event characteristic (in particular it does not depend on the lens mass). On the other hand, the microlensing rate allows one to make estimates on the expected number of events and their characteristics (in particular of the duration, that is linked to the lens mass).

##### 3.2.1 The optical depth

Maps for the microlensing optical depth towards the LMC have been obtained and discussed in a number of papers (e.g. Mancini et al. 2004). Following the LMC structure, the LMC self-lensing (LMC disc or bar sources *and* lenses) optical depth is symmetric around the LMC centre and peaks at  $\tau = 5 \times 10^{-8}$ . Most of the area covered by the OGLE-II fields is within the line of equal optical depth above  $\tau = 2 \times 10^{-8}$ . The Galactic dark matter halo optical depth, on the other hand, is a very smoothly varying function of the position across the LMC, with the lines of equal optical

depth roughly parallel to the LMC bar axis, and typical value within the OGLE-II fields of  $\tau = (44 - 45) \times 10^{-8}$ . In Fig. 1 we show the maps of the optical depth for these two lens populations together with the location of the OGLE-II fields and the position of the observed events. As for the Galactic disc optical depth, this also turns out to be a smoothly varying function of the position, with typical value along the LMC bar down to 10 times as small as the LMC self lensing, with typical value of  $\tau \sim 0.40 \times 10^{-8}$ . On the other hand, the LMC dark matter halo optical depth (Mancini et al. 2004) shows a strong variation with the position, also due to the inclination of the LMC disc. Along the LMC bar it results  $\tau \sim 6 \times 10^{-8}$ . In Table 2 we report the values of the optical depth for all the LMC lens populations considered along the lines of sight towards the 21 OGLE-II fields and the two microlensing candidate events. The LMC stellar halo optical depth is strongly enhanced, in particular towards the central LMC region, when using the Pejcha & Stanek (2009) triaxial model as opposed to the spherical one of Alves (2004). Nevertheless, this contribution remain small with respect to the LMC self lensing. As for the Galactic stellar lensing, the contribution of the disc and the stellar halo turn out to be rather negligible with respect to the LMC self lensing, and this holds in particular because all of the observed fields are concentrated along the LMC bar region. For the Galactic disc and stellar halo we find  $\tau \sim 0.4 \times 10^{-8}$  and  $\tau \sim 0.2 \times 10^{-8}$ , respectively.

As for the line of sight towards the OGLE-II observed events, both of them happen to fall within the line of equal LMC self-lensing optical depth of  $\tau = 3.0 \times 10^{-8}$  (upper panel of Fig. 1), with the innermost event within that of  $\tau = 4.5 \times 10^{-8}$ . These values compare well with the overall observed estimate  $\tau_{\text{obs}} = (4.3 \pm 3.3) \times 10^{-8}$ .

### 3.2.2 The microlensing rate

We have evaluated the microlensing rate along the lines of sight towards the 21 fields observed during the OGLE-II campaign for the different lens populations we consider. We have made use of the detection efficiency evaluated as described in Wyrzykowski et al. (2009) for both the *All* and the *Bright* samples of sources to take into account of the observational effects. Coherently with the analysis of Wyrzykowski et al. (2009), we reduce the efficiency by a factor 0.9 to take into account binary systems that might be missed by the pipeline. To evaluate the differential microlensing rate we have included, beside the random component of the velocity, the bulk motion of the LMC and of the observer and the drift velocity of the LMC disc following the scheme outlined in Calchi Novati et al. (2006).

In Table 3 we report the main result of the present analysis on the expected microlensing signal: the median value of the duration and the number of events,  $n_{\text{exp}}$ . As for the *All* sample of sources, the expectations for  $n_{\text{exp}}$  from the luminous lens populations sum up roughly to 1.5 events, with more than 70% of the lensing signal expected from the LMC self lensing. This compares well with the observed number of events  $n_{\text{obs}} = 2$ . The prediction for the number of expected events for the restricted bright sample,  $\sim 0.65$  events, is also fully compatible with the null result obtained in this case. As it follows from the location of the observed fields, we can also see that the expected signal from the Galactic disc is significantly smaller as compared to the LMC self-lensing one.

For the LMC stellar halo lensing we have considered here the fiducial spherical Alves (2004) model. In fact the number of expected events using the Pejcha & Stanek (2009) triaxial model increases significantly, by about 50%. However, this contribution re-

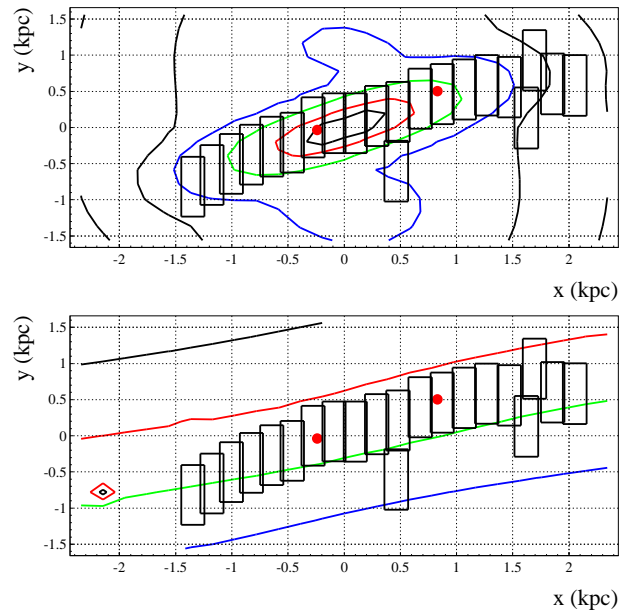


**Figure 1.** Maps of microlensing optical depth towards the LMC: LMC self lensing (upper panel) and Galactic dark matter halo. The contours indicate the lines of equal optical depth corresponding to the values  $\tau = (1.0, 1.5, 2.0, 3.0, 4.0, 4.5) \times 10^{-8}$  (upper panel) and  $\tau = (43, 44, 45, 46) \times 10^{-8}$ . The boxes indicate the position of the 21 fields monitored during the OGLE-II campaigns. The filled circles mark the position of the two observed OGLE-II candidate microlensing events. The  $x - y$  reference system has its origin at the centre of the LMC, the  $x$ -axis antiparallel to the right ascension and the  $y$ -axis parallel to the declination.

mains small with respect to that of the LMC self lensing, so that the overall increase is of only about 6% and our overall conclusion are not significantly changed when using one model or the other.

Analogously, one might consider the same triaxial spatial distribution, elongated along the line of sight, also for the dark matter LMC halo. As we have shown to be the case for the stellar one, we may expect the optical depth, and correspondingly the microlensing rate, to increase significantly, mainly because of the increased mean lens-source distance. However, since the ratio of LMC over Galactic compact halo objects rate is quite small, less than 10% (Table 3), we do not expect our results to be significantly affected by this choice. This is the case also because of the small statistics of events at disposal. A larger set would allow one a study of the spatial distribution, too, and in that case a different spatial distribution for the LMC halo contribution might become a relevant issue (Calchi Novati et al. 2006).

The expected duration varies across the observed fields for the LMC self lensing, with larger values expected moving from the LMC centre, with variations up to about 10% (Mancini et al. 2004). In Table 3 we have reported the mean values of the duration across the 21 OGLE fields. In particular, as for the lines of sight towards the two candidates it results a median (average) value  $t_E = 36$  (49) days and  $t_E = 47$  (61) days, to be compared with the observed values  $t_E = 57.2$  days and  $t_E = 24.2$  days, for OGLE-LMC-I and OGLE-LMC-II, respectively.

In Fig. 2 we show the normalised differential rate  $d\Gamma_{\mathcal{E}}/dt_E$ , corrected for the efficiency  $\mathcal{E}(t_E)$ , for LMC self lensing and for Galactic dark matter halo lenses of  $0.1 M_{\odot}$  and  $1 M_{\odot}$ . Superimposed on the differential rate we show the values of the eval-

**Table 3.** Results of the microlensing rate analysis for the different lens populations we consider: evaluation of the duration and number of expected events,  $n_{\text{exp}}$  as evaluated on the 21 fields monitored during the OGLE-II campaign. For the Einstein time we report the values averaged across the observed fields. For  $n_{\text{exp}}$  we report the sum over the observed fields, taking into account the efficiency, for both the *All* and the *Bright* sample of sources. SL and SH stand for self lensing and stellar halo, respectively.

lenses	$t_E$			$n_{\text{exp}}$	
	16%	50%	84%	<i>All</i>	<i>Bright</i>
LMC SL	26.	52.	100.	1.1	0.46
LMC SH	24.	46.	83.	0.20	0.086
MW disc	18.	34.	65.	0.12	0.056
MW SH	19.	34.	65.	0.071	0.031
MW halo					
$10^{-5} M_\odot$	3.2	4.7	11.	0.40	0.19
$10^{-4} M_\odot$	3.3	4.8	11.	3.3	1.6
$10^{-3} M_\odot$	3.5	5.5	12.	12.	5.0
$10^{-2} M_\odot$	6.3.	9.7	18.	21.	9.2
0.1 $M_\odot$	13.	20.	36.	27.	12.
0.5 $M_\odot$	25.	40.	69.	18.	7.7
1.0 $M_\odot$	33.	56.	94.	14.	6.0
10 $M_\odot$	91.	150.	230.	4.3	2.0
LMC halo					
$10^{-5} M_\odot$	3.2	4.7.	11.	0.15	0.071
$10^{-4} M_\odot$	3.3	4.9	11.	1.1	0.48
$10^{-3} M_\odot$	3.6	6.5	11.	2.1	0.91
$10^{-2} M_\odot$	9.3	14.	23.	3.9	1.7
0.1 $M_\odot$	22.	35.	57.	2.9	1.2
0.5 $M_\odot$	47.	74.	120.	1.5	0.68
1.0 $M_\odot$	63.	100.	160.	1.1	0.50
10 $M_\odot$	160.	250.	340.	0.22	0.10

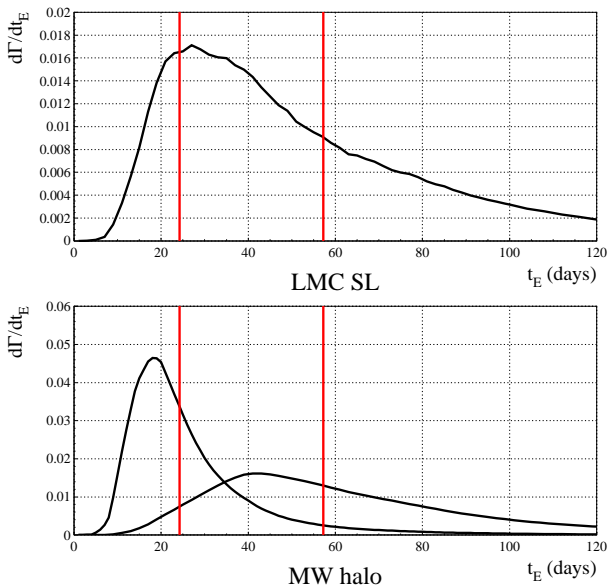


**Figure 2.** Normalised microlensing differential rate  $d\Gamma_{\mathcal{E}}/dt_E$  towards the LMC corrected for the OGLE-II efficiency: LMC self lensing (upper panel) and Galactic dark matter halo (0.1 and 1  $M_\odot$ , the former peaked at lower values of the duration). The vertical solid lines indicate the value of the duration of the two observed OGLE-II events.

uated duration for the two events observed using the *All* sample of sources. Comparing the expected durations with the observed ones we can see, as for self lensing, that the evaluated duration of OGLE-LMC-1 agrees very well with the median value, and, though somewhat short, that of OGLE-LMC-2, is still fully compatible. As for the MW MACHO populations, the observed durations are compatible with those expected for MACHO masses in the mass range  $(0.1 - 1) M_\odot$ .

The expected number of events for the dark populations (both MW and LMC halos) is shown, as a function of the MACHO mass, in the upper panel of Fig. 3. In particular, for a full halo of  $0.05 M_\odot$  ( $0.5 M_\odot$ ) compact objects we expect, for the MW halo,  $n_{\text{exp}} = 28$  and  $n_{\text{exp}} = 12$  ( $n_{\text{exp}} = 18$  and  $7.7$ ) for the *All* and the *Bright* sample of sources, respectively, whereas for the LMC halo we evaluate  $n_{\text{exp}} = 3.5$  and  $n_{\text{exp}} = 1.5$  ( $n_{\text{exp}} = 1.5$  and  $0.68$ ). For both MW and LMC, the microlensing rate is severely suppressed by the sharp decline of the efficiency function  $\mathcal{E}(t_E)$  (Wyrzykowski et al. 2009) for small values of  $t_E$ : this explains the plateau reached by the expected duration values, as well as the sharp decline for  $n_{\text{exp}}$ , for compact halo object masses below  $10^{-3} M_\odot$ .

### 3.3 The mass halo fraction in form of MACHOs

The evaluation of the microlensing rate together with the result of the OGLE-II observational campaign as for the number of observed microlensing events allows us to put some constraints on the mass halo fraction in form of MACHOs,  $f$ . In particular we perform a likelihood analysis with

$$L(f, m) = \exp(-N_{\text{exp}}(f, m)) \prod_{i=1}^{N_{\text{obs}}} \left. \frac{d\Gamma_{i,\mathcal{E}}}{dt_E} \right|_{t_{E,\text{event}}}, \quad (1)$$

where, for the differential rate, we sum up over all the luminous and dark populations we consider. The halo mass fraction,  $f$ , enters as a multiplicative factor of the differential rate and of the expected number of events in front of the contribution of the dark populations (MW and LMC halos).

Keeping the MACHO mass value fixed as a parameter we can evaluate upper and lower limits for the halo mass fraction  $f$ . In Fig. 3 (bottom panel) we display the 90% and 95% confidence levels *upper* limits for  $f$ , for both the *All* sample and the *Bright* sample (thick and thin lines, respectively). As noted in the previous Section, the number of expected events from the luminous lens components is compatible with the observed one in both cases, therefore we do not show the corresponding (extremely small) lower limit. Corresponding to the maximum in the number of MACHO events (upper panel, Fig. 3), we find the tighter constraints for the halo component in form of MACHOs in the mass range  $(10^{-2} - 10^{-1}) M_\odot$ . For  $0.05 M_\odot$  MACHOs we find, at the 90% (95%) confidence levels,  $f < 11\%$  ( $14\%$ ) for the *All* sample and  $f < 17\%$  ( $22\%$ ) for the *Bright* sample. Finally, for a MACHO mass of  $0.5 M_\odot$ , about the value preferred by the MACHO collaboration analyses, we find  $f < 21\%$  ( $26\%$ ) (*All* sample) and  $f < 27\%$  ( $36\%$ ) (*Bright* sample).

We may compare these results with those obtained under the assumption of  $n_{\text{obs}} = 0$  with a confidence limit analysis based on a Poisson distribution for the number of expected MACHO lensing events (as that carried out in Wyrzykowski et al. 2009). The analysis yields the same results for the *Bright* sample ( $n_{\text{obs}} = 0$ ) but a few differences arise for the *All* sample ( $n_{\text{obs}} = 2$ ), where we are including the information on the observed events, and in partic-

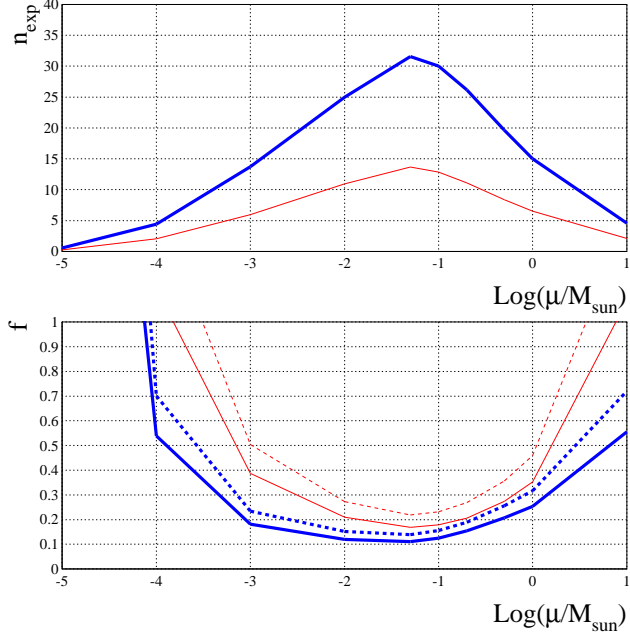


**Figure 3.** Upper panel: number of expected events for (full) dark matter halos (MW and LMC). Bottom panel: as a result of the likelihood analysis, 90% and 95% confidence level (solid and dashed lines, respectively) upper limits for the halo mass fraction in form of compact halo objects. The tick and thin lines indicate the results for the *All* ( $n_{\text{obs}} = 2$ ) and the *Bright* ( $n_{\text{obs}} = 0$ ) sample of sources, respectively. The number of expected events from the luminous populations is  $n_{\text{exp}} = 1.5$  and  $n_{\text{exp}} = 0.65$ , respectively.

ular of their timescale, and that on the expected number of events from the luminous populations. For the *All* sample we expect the limits to rise whenever the observed durations fit well the expected ones for the dark matter components. For MW compact halo objects this holds in the mass range  $(10^{-1} - 1) M_{\odot}$  (Table 3, Fig. 2). In particular, for a dark matter halo of compact objects of  $0.5 M_{\odot}$  with the simpler Poisson analysis we obtain  $f < 12\%$  ( $15\%$ ) at the 90% and 95% confidence levels<sup>1</sup>, respectively, to be compared with  $f < 21\%$  ( $26\%$ ).

Finally, we can integrate over the mass the expression of the likelihood in the full range considered ( $(10^{-5} - 10) M_{\odot}$ ) and, by Bayesian inversion, obtain the one dimensional probability distribution for the halo mass fraction,  $P(f)$ . Here we use a  $d \log(\mu_l)$  prior on the mass (but the results are similar, with a resulting distribution just somewhat broader, for a flat prior  $d(\mu_l)$ ). We show the halo mass fraction in form of MACHOs probability distribution,  $P(f)$ , together with the corresponding cumulative distribution,  $D(f)$ , in Fig. 4.

Although, as discussed, the expected microlensing signal contributed by the luminous lens populations is sufficient to explain the observed events, in principle it is possible to take the opposite view, namely that the luminous populations *do not* contribute to the microlensing rate. In this case we may evaluate, for the *All* sample, what halo fraction is implied by the two observed events, and it

<sup>1</sup> The results we obtain are somewhat different from those reported in Wyrzykowski et al. (2009), where the analysis was based on a few approximations. In particular for  $0.4 M_{\odot}$  MACHOs we evaluate an upper limit  $f < 14\%$  at 95% confidence level.

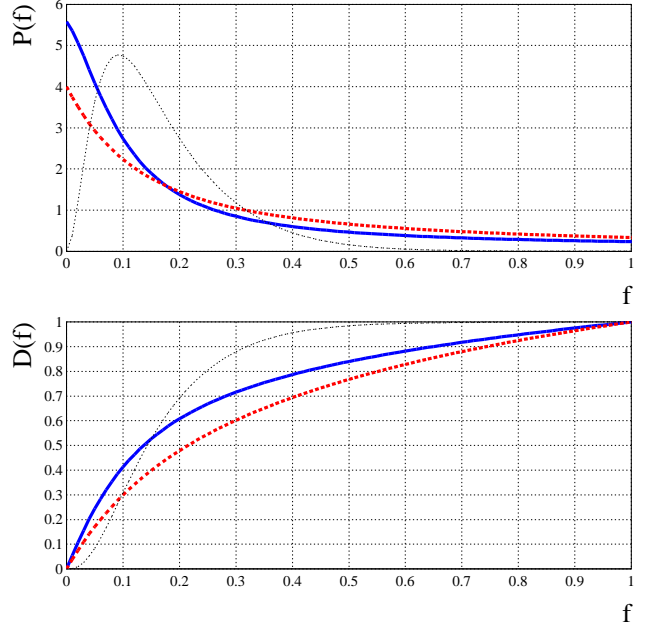


**Figure 4.** Probability (upper panel) and cumulative distribution for  $f$ , the halo mass fraction in form of MACHOs, obtained after integration on the MACHO mass with a logarithmic flat prior of the likelihood function. The solid (dashed) lines are for the *All* ( $n_{\text{obs}} = 2$ ) and the *Bright* ( $n_{\text{obs}} = 0$ ) sample of sources, respectively. The (thinner) dotted line, for the *All* sample, is obtained neglecting the contribution to the microlensing rate of the luminous populations, namely, assuming that the observed events are due to MACHOs.

therefore makes sense to evaluate both an upper and a lower limit for  $f$ . This can be looked at as the extreme case (opposite to the Poisson-based analysis with  $n_{\text{obs}} = 0$ ) that fixes the limits that can be put on the MACHO contribution. The resulting probability distribution for  $f$ , together with the cumulative distribution, is shown in Fig. 4: the halo fraction peaks at  $f \sim 10\%$  with a dispersion of about 8%. In particular, for a  $0.5 M_{\odot}$  compact halo objects halo we find lower and upper limits for  $f$  of 4% and 32% (95% confidence level).

## 4 CONCLUSION

In this paper we have analysed the recent results presented by the OGLE collaboration as for their OGLE-II campaign directed towards the bar region of the LMC (Wyrzykowski et al. 2009). In particular we have carried out a detailed analysis of the expected signal from the luminous lens populations (LMC bar, disc and stellar halo, MW disc and stellar halo) as compared to MACHO lensing (LMC and MW dark matter halos).

The overall conclusion of our analyses, in agreement with that reported in Wyrzykowski et al. (2009), is that the observed signal is in full agreement with that expected from the luminous components (largely dominated by the LMC self lensing). This holds looking both at the duration and at the number of the observed events. The relatively small statistic at disposal, however, does not allow at the same time to put very strong constraints on the contribution to the halo in form of compact halo objects. Indeed the evaluated upper limit for the halo mass fraction in form of MACHOs,  $f$ , is still, even if only marginally, consistent with the positive MACHO signal



reported by the MACHO collaboration. On the other hand, it is much less severe than that reported by the EROS collaboration.

In particular, the estimated value for the optical depth for the two observed events  $\tau_{\text{obs}} = (4.3 \pm 3.3) \times 10^{-8}$ , compares well with our estimate of  $\tau$  for LMC self lensing: both events lie within the line of equal optical depth  $\tau = 3.0 \times 10^{-8}$ , with the innermost one within that of  $\tau = 4.5 \times 10^{-8}$ . Furthermore, through the evaluation of the microlensing rate, we have shown that the observed signal, 2 events with duration in the range 20-60 days, is compatible with the expected signal from the luminous lens components, with  $n_{\text{exp}} = 1.5$  and a typical duration, for LMC self lensing, of 50 days. As for the halo mass fraction in form of MACHOs, given the agreement of the observed signal with self lensing, we report an *upper* limit only. Through a likelihood analysis we have evaluated an *upper* limit for  $f$  at 95% confidence level as low as 14% for compact objects of  $0.05 M_{\odot}$  and values varying in the range 16%-32% in the mass range  $(0.1 - 1) M_{\odot}$ , that preferred by the analyses of the MACHO group (and for which the expected durations of the would be Galactic MACHO populations are in agreement with the observed ones).

The OGLE-II campaign sampled the bar region of the LMC only. Together with the low statistics of observed events this makes more difficult the task of disentangling the would be MACHO lensing from the lensing signal due to the luminous lens populations. In fact, a larger number of observed events is crucial to this purpose as it may allow one analyses such those carried out in Mancini et al. (2004) and Calchi Novati et al. (2006) on the duration and the spatial distribution of the events. The upcoming results of the OGLE-III campaign, together with those of SuperMACHO (Rest et al. 2005), which both covered a larger area of the sky with an expected larger statistics of events, should eventually allow one to put further constraints on the distribution of the dark matter halo in form of MACHOs.

#### ACKNOWLEDGMENTS

SCN acknowledges support from the Italian Space Agency (ASI). SCN, LM and GS acknowledge support by FARB-2009 of the University of Salerno. LW acknowledges generous support from the European Community's FR6 Marie Curie Programme, Contract No. MRTN-CT-2004-505183 "ANGLES" and EC FR7 grant PERG04-GA-2008-234784.

#### REFERENCES

Alcock C., Akerloff C. W., Allsman R. A., Axelrod T. S., et al., 1993, *Nature*, 365, 621  
 Alcock C., Allsman R. A., Alves D. R., Axelrod T. S., et al., 2000, *ApJ*, 542, 281  
 Alcock C., Allsman R. A., Alves D. R., Axelrod T. S., et al., 2001, *Nature*, 414, 617  
 Alves D. R., 2004, *ApJ*, 601, L151  
 Aubourg E., Bareyre P., Brehin S., Gros M., et al., 1993, *Nature*, 365, 623  
 Bennett D. P., 2005, *ApJ*, 633, 906  
 Borissova J., Minniti D., Rejkuba M., Alves D., 2006, *A&A*, 460, 459  
 Calchi Novati S., de Luca F., Jetzer P., Mancini L., Scarpetta G., 2008, *A&A*, 480, 723

Calchi Novati S., De Luca F., Jetzer P., Scarpetta G., 2006, *A&A*, 459, 407  
 Chabrier G., 2003, *PASP*, 115, 763  
 Cole A. A., Tolstoy E., Gallagher III J. S., Smecker-Hane T. A., 2005, *AJ*, 129, 1465  
 Da Rio N., Gouliermis D., Henning T., 2009, arXiv:0902.0758  
 Dong S., Udalski A., Gould A., Reach W. T., et al., 2007, *ApJ*, 664, 862  
 Gillessen S., Eisenhauer F., Trippe S., Alexander T., et al., 2009, *ApJ*, 692, 1075  
 Gouliermis D., Brandner W., Henning T., 2006, *ApJ*, 641, 838  
 Groenewegen M. A. T., Udalski A., Bono G., 2008, *A&A*, 481, 441  
 Gyuk G., Dalal N., Griest K., 2000, *ApJ*, 535, 90  
 Hamadache C., Le Guillou L., Tisserand P., Afonso C., et al. 2006, *A&A*, 454, 185  
 Han C., Gould A., 2003, *ApJ*, 592, 172  
 Helmi A., 2008, *A&ARv*, 15, 145  
 Jetzer P., Mancini L., Scarpetta G., 2002, *A&A*, 393, 129  
 Kallivayalil N., Patten B. M., Marengo M., Alcock C., Werner M. W., Fazio G. G., 2006, *ApJ*, 652, L97  
 Kroupa P., 2002, *Science*, 295, 82  
 Kroupa P., 2007, astro-ph/0703124  
 Kroupa P., 2008, in Aarseth S. J., Tout C. A., Mardling R. A., eds, *Lecture Notes in Physics*, Berlin Springer Verlag Vol. 760, p 181, arXiv:0803.1833  
 Mancini L., 2009, *A&A*, 496, 465  
 Mancini L., Calchi Novati S., Jetzer P., Scarpetta G., 2004, *A&A*, 427, 61  
 Minniti D., Borissova J., Rejkuba M., Alves D. R., Cook K. H., Freeman K. C., 2003, *Science*, 301, 1508  
 Paczyński B., 1986, *ApJ*, 304, 1  
 Paczyński B., 1991, *ApJ*, 371, L63  
 Pejcha O., Stanek K., 2009, arXiv:0905.3389  
 Popowski P., Griest K., Thomas C. L., Cook K. H., et al. 2005, *ApJ*, 631, 879  
 Rest A., Stubbs C., Becker A. C., Miknaitis G. A., et al. 2005, *ApJ*, 634, 1103  
 Roulet E., Mollerach S., 1997, *Phys. Rep.*, 279, 67  
 Sahu K. C., 1994, *Nature*, 370, 275  
 Subramaniam A., 2005, *A&A*, 430, 421  
 Sumi T., Woźniak P. R., Udalski A., Szymański M., et al. 2006, *ApJ*, 636, 240  
 Thies I., Kroupa P., 2007, *ApJ*, 671, 767  
 Tisserand P., Le Guillou L., Afonso C., Albert J. N., et al., *The EROS-2 Collaboration* 2007, *A&A*, 469, 387  
 Trippe S., Gillessen S., Gerhard O. E., Bartko H., et al., 2008, *A&A*, 492, 419  
 Udalski A., Szymanski M., Kaluzny J., Kubiak M., et al., 1993, *Acta Astronomica*, 43, 289  
 van der Marel R. P., Cioni M.-R. L., 2001, *AJ*, 122, 1807  
 van der Marel R. P., 2001, *AJ*, 122, 1827  
 van der Marel R. P., Alves D. R., Hardy E., Suntzeff N. B., 2002, *AJ*, 124, 2639  
 Wu X.-P., 1994, *ApJ*, 435, 66  
 Wyrzykowski L., Kozłowski S., Skowron J., Belokurov V., et al., 2009, *MNRAS*, 397, 1228  
 Zhao H., Evans N. W., 2000, *ApJ*, 545, L35